Summer frontal contribution to the fertilization of oceanic waters off the northeast coast of Spain

Western Mediterranean
Cross frontal circulation
Fertilization
Particle size
Coulter counter
Méditerranée occidentale
Fronts
Fertilisation
Particules
Compteur Coulter

Jordi FLOS [a], **Joaquin TINTORÉ** [b]
[a] Departament d'Ecologia, Universitat de Barcelona, Diagonal 645, 08028 Barcelona, Spain.
[b] Departament de Fisica, Universitat de Les Illes Balears, 07071 Palma de Mallorca, Spain.

Received 11/4/88, in revised form 30/5/89, accepted 7/6/89.

ABSTRACT

The physical, biological and chemical structures detected in July 1983 between the northeast coast of the Iberian peninsula and the Balearic Islands are analysed and discussed in this paper. Principal component analysis and cluster analysis are used to sumarize the information. Evidence of the contribution of the cross-frontal circulation to the biological fertilization of the offshore regions is presented and discussed. It is also suggested that offshore jets or filaments of low-salinity coastal water strongly enhance the diapycnal mixing that is responsible for the upward transport of nutrients on the offshore side of the shelf/slope front.

Oceanologica Acta, 1990. **13**, 1, 21-30.

RÉSUMÉ

Front estival et fertilisation des eaux du large au nord-est de l'Espagne

Les structures physiques, biologiques et chimiques des eaux ont été observées, en juillet 1983, entre la côte nord-est de la péninsule ibérique et les îles Baléares. Les données, traitées par analyse en composantes principales et analyse des groupes, mettent en évidence le rôle de la circulation à travers le front dans la fertilisation biologique des eaux du large. Il est suggéré que les filaments d'eau côtière peu salée renforcent le mélange diapycne responsable de l'apport de sels nutritifs par les eaux du large qui remontent le long du front.

Oceanologica Acta, 1990. **13**, 1, 21-30.

INTRODUCTION

Biologically, the Mediterranean is known for its oligotrophic character, but the relatively high abundance of a variety of animals in the higher trophic levels prompted Sournia (1973) to talk about the paradox of the Mediterranean. Seeking the missing production that could explain this paradoxal situation, biologists have focused their attention on the ratio of new and regenerated production (Dugdale and Goering, 1967) to total production.

Classical works on the geostrophic circulation of the Western Mediterranean (Alain, 1960; Ovchinnikov, 1966) introduced the idea of a central upward lift of isopycnals (often called central dome or divergence) extending from the Ligurian Sea to the southern part of the Balearic Sea. This widely accepted idea of central divergence with its associated cyclonic circulation was thought to be the main enrichment mechanism of the region, responsible for all new production that had not been previously accounted for (Jacques *et al.*, 1973; 1976).

A new picture of the circulation of the Balearic Sea has recently emerged. Font *et al.* (1988) discuss the existence of this permanent doming structure but relate it to the existence of two density fronts, one over the continental slope region and the other northwest of the Balearic Islands. La Violette *et al.* (1990), in an extensive analysis of satellite imagery, showed the importance of these two frontal features to the surface circulation in the Balearic Sea.

The fertilizing mechanisms supplying nutrients to the photic zone were discussed by Estrada and Margalef

(1988), who distinguished the following mechanisms: 1) local mixing due to the breakdown of the thermocline; 2) wind-induced upwelling at the slope region; 3) surface influx of modified Atlantic water; 4) river runoff; and 5) frontal contribution. It is important to note that Estrada and Margalef (1988) defined frontal contribution as the upward motion of nutrients in the central, almost permanent, doming structure.

In this paper we present evidence of summer enrichment associated with the shelf/slope front off the northeast Spanish coast. We discuss the vertical motions induced by the different physical features and their biological implications.

DATA AND METHODS

Data were collected on board the R/V Garcia del Cid from 30 June to 16 July 1983 in a region between Barcelona and Mallorca (Fig. 1). An intense survey of the shelf/slope region off Barcelona was carried out between 30 June and 3 July. The data included CTD casts and Niskin bottles, from which chlorophyll, coulter counter seston, nitrate, nitrite, oxygen, reactive phosphate and silicate were analysed (Grup PEPS, 1986). Principal component analysis (*i.e.* Legendre and Legendre, 1983) is used to summarize hydrographic data (Flos, 1979; 1980) and particle size spectra (Kitchen *et al.*, 1975; Flos, 1976). A cluster analysis of the samples was applied using the values from the first two PCA as descriptors.

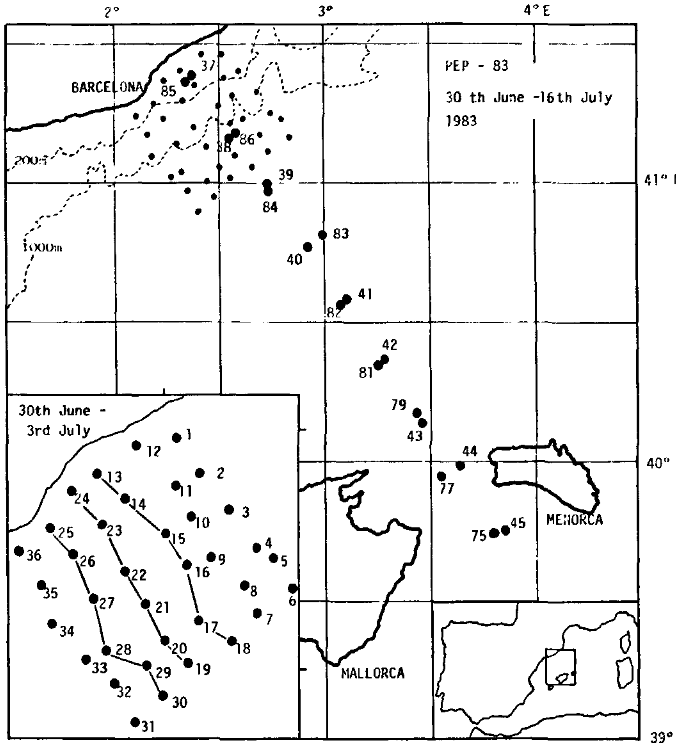

Figure 1

Map distribution of stations. On the left, enlargement of the 36 coastal stations with indication of the transects shown in other figures.

Situation des stations. En cartouche : les 36 stations côtières, avec indication des coupes transversales présentées dans les autres figures.

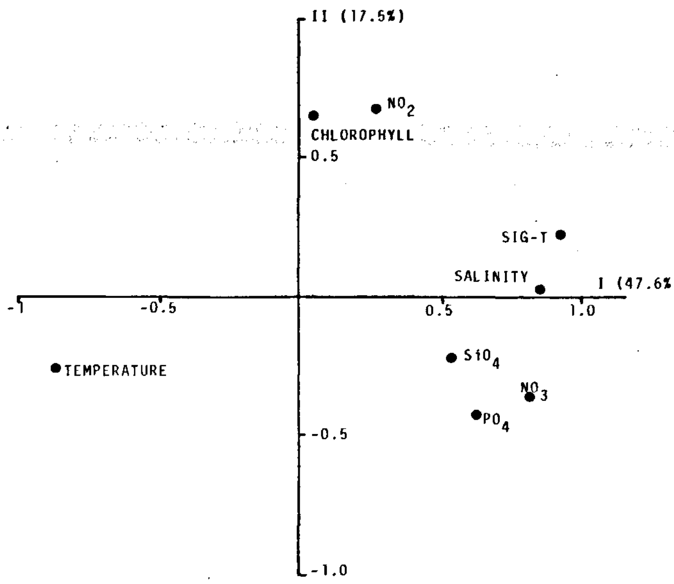

Figure 2

Principal component analysis of hydrographical data. Distributions of variables are shown in the two first principal axes. Percentage of explained variance is also shown.

Analyse en composantes principales des données hydrologiques. Distribution des variables dans le plan des deux premiers axes. Le pourcentage de la variance exprimée par chaque axe est indiqué entre parenthèses.

Principal component analysis of hydrographic data

In the principal component analysis we used temperature, salinity, sigma-t, nitrate, nitrite, phosphate, silicate and chlorophyll a (logarithmic transformation). Oxygen was not included because of insufficient data. The correlation matrix was computed using 793 samples, one-third of which belonged to the coastal grid (Fig. 1). Only two eigen vectors were greater than unity (3.81 and 1.40), accounting for 65 % of the variance (47.5 and 17.5 % respectively). The first component was well correlated with temperature, salinity, sigma-t and nutrients and reflects the importance of stratification and vertical segregation of nutrients. The second component was mainly due to the coincidence of chlorophyll and nitrite maxima at intermediate levels (Fig. 2 and 7). It reflects the biological activity at depths where vertical density and nutrient gradients are present and where irradiance permits the persistence and/or growth of phytoplankton (Fig. 3). This result is typical for Mediterranean waters in the stratified season (Flos, 1980). The same analysis performed without sigma-t as a variable shows no difference for the second component, and reduces by 12 % the variance calculated for the first one.

Principal component analysis of seston data

In this study, we used particulate volumes measured in 14 size intervals (from 3.5 to 70.6 µm mean equivalent particle diameters, corresponding to coulter counter channels, *see e.g.* Sheldon and Parsons, 1967). Three eigen values greater than unity were obtained, accounting for 82.8 % of the variance (58.3, 15.3 and 9.2 % respectively). Positive scores for the first component

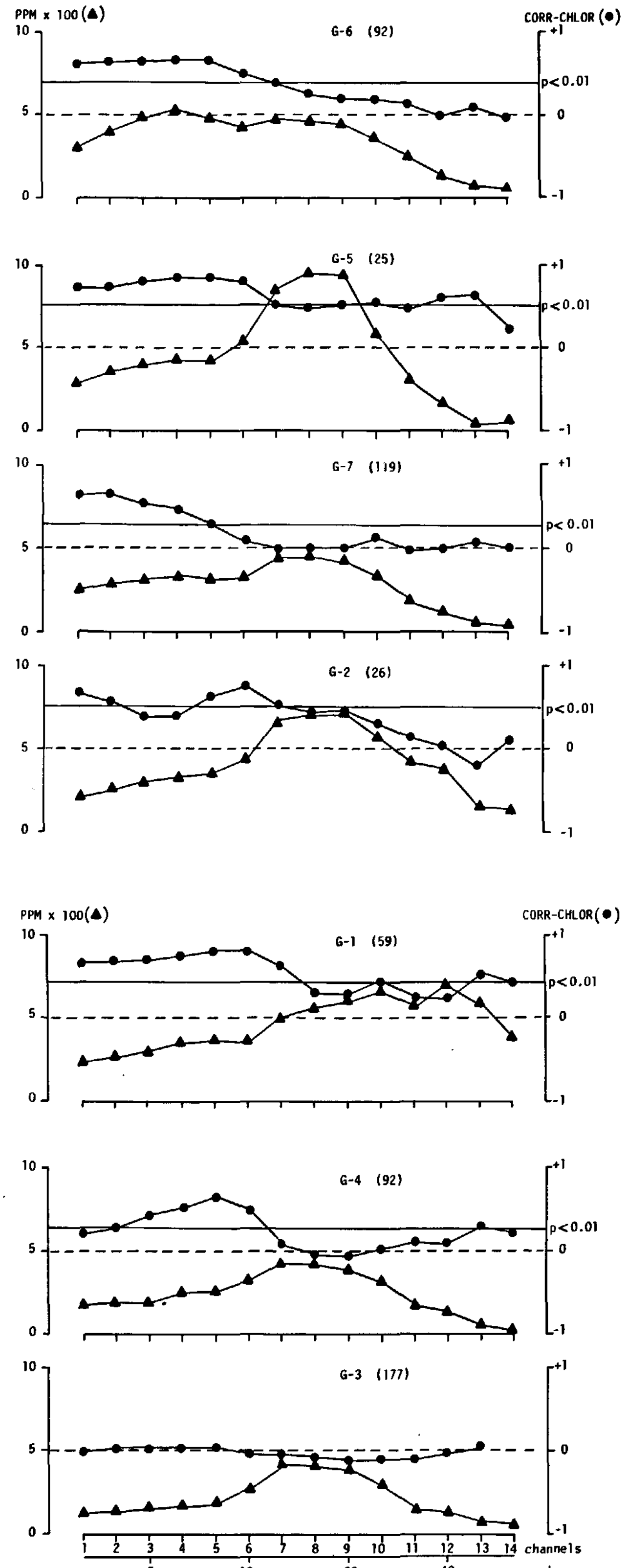

Figure 3

Mean size spectra for each of the seven groups of samples retained after cluster analysis (triangles: ppm × 100, scale on the left). Within-group correlation between particle volume in each size interval and chlorophyll (dots: correlation scale on the right; significance level of $p < 0.01$ indicated). The number of samples in each group is given in parentheses.

Spectre de taille moyenne pour chacun des sept groupes d'échantillons trouvés par l'analyse de groupes (triangles : l'échelle des ordonnées est en ppm × 100). Le coefficient de corrélation entre le volume de chaque intervalle et la chlorophylle calculée pour le groupe (points : échelle à droite; ligne horizontale : niveau de probabilité $p < 0.01$). En haut : numéro du groupe et nombre d'échantillons, entre parenthèses.

are equivalent to high total volume of seston, being particles with an equivalent diameter around 10 µm highly correlated with the first component. The other two factors combined indicate the size frequency distribution. Positive scores for the second factor are related to particles between 20 and 35 µm; negative values are related to smaller particles (less than 7 µm). Positive values for the third factor are related to particles greater than 35 µm, and negative values to particles around 15 µm.

Cluster analysis

We clustered the 164 samples of the first 36 stations using as descriptors the scores issued from the former PCA of hydrographic and seston data (2 and 3 scores respectively). The Euclidean distance was used and the aggregation algorithm was that of Ward (1963). We obtained 7 groups of samples by cutting the dendrogram at an arbitrary level of similarity (which gave us a sizeable number of clusters). A discriminant analysis (SPSSX package) was used to assess the clustering procedure (resulting 92.7 % of the samples well classified) and to classify samples from other stations that had not entered the cluster analysis.

Means and standard deviations of original hydrographic and seston variables were computed for every group (Table). We also computed, for each group, the correlation between chlorophyll and the volume of seston of the different size intervals (Fig. 3).

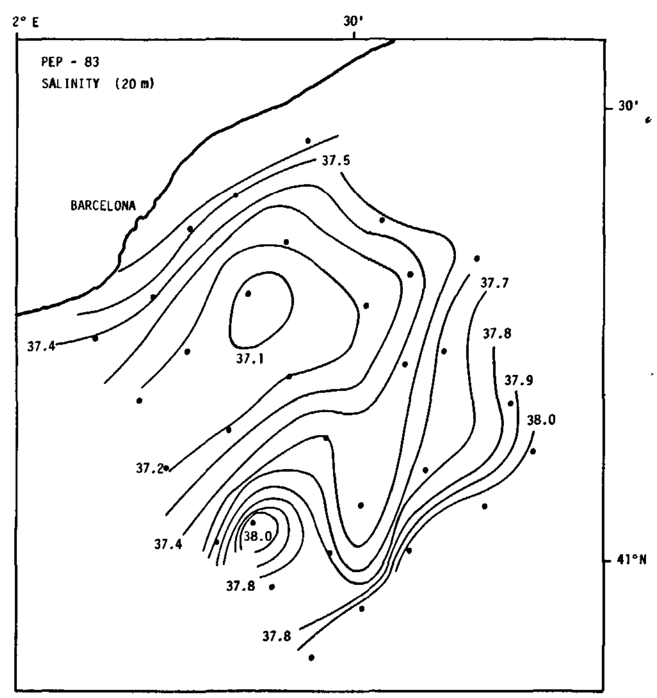

Figure 4

Horizontal distribution of salinity at 20 m depth on the coastal grid of stations.

Répartition horizontale de la salinité à 20 m de profondeur pour les stations du réseau côtier.

Table

Group means and standard deviations for depth, temperature, salinity, sigma-t, oxygen (ml/l), amonium, nitrite, nitrate, silicate, phosphate (µM), chlorophyll a *(µg/l), total number of particles (in thousands per mililitre) and total volum of seston (ppm). Number of samples in each group is indicated on the top.*

Pour chaque groupe, moyenne et écarts-type des variables : profondeur, température, salinité, sigma-*t*, oxygène (ml/l), amonium, nitrite, nitrate, silicate, phosphate (µM), chlorophylle *a* (µg/l), nombre total de particules (milliers par millitre) et volume total de seston (ppm). Le nombre d'échantillons dans chaque groupe est indiqué en haut.

	Groups						
	1	2	3	4	5	6	7
Samples	59	26	177	92	25	92	119
Depth	63.6 ±18.7	45.2 ±16.5	152.7 ±139.1	75.4 ±15.9	24.2 ±17.6	8.9 ±9.0	45.6 ±15.1
Temperature	14.2 ± 1.3	15.8 ± 1.9	13.1 ± 0.2	13.7 ± 1.0	18.7 ± 1.8	21.9 ±2.2	15.9 ± 1.7
Salinity	37.97± 0.26	37.87± 0.31	38.29± 0.12	38.11± 0.16	37.55± 0.36	37.61±0.33	37.94± 0.26
Sig-*t*	28.47± 0.46	28.02± 0.63	28.95± 0.12	28.68± 0.34	27.07± 0.62	26.22±0.60	28.05± 0.53
Oxygen	5.55± 0.38	5.50± 0.22	4.91± 0.33	5.27± 0.28	5.33± 0.31	5.17±0.34	5.68± 0.35
Ammonium	0.11± 0..07	0.16± 0.11	0.10± 0.07	0.10± 0.06	0.11± 0.07	0.13±0.09	0.11± 0.08
Nitrite	0.04± 0.06	0.03± 0.04	0.04± 0.04	0.18± 0.09	0.02± 0.04	0.01±0.01	0.02± 0.03
Nitrate	0.65± 1.15	0.13± 0.17	5.09± 1.31	1.54± 0.88	0.12± 0.13	0.06±0.10	0.07± 0.11
Silicate	1.00± 0.81	0.70± 0.51	3.28± 1.40	1.54± 0.77	0.52± 0.49	0.21±0.28	0.83± 0.71
Phosphate	0.11± 0.16	0.10± 0.07	0.28± 0.15	0.10± 0.09	0.13± 0.11	0.06±0.08	0.06± 0.07
Chlorophyll	0.77± 0.94	0.52± 0.43	0.30± 0.69	0.84± 0.78	0.54± 0.70	0.15±0.08	0.46± 0.38
N. part	2.22± 1.25	2.52± 0.74	0.96± 0.48	1.87± 0.95	3.31± 1.37	2.10±0.78	2.22± 0.79
V. part	0.54± 0.32	0.59± 0.16	0.23± 0.11	0.33± 0.13	0.73± 0.34	0.34±0.13	0.35± 0.10

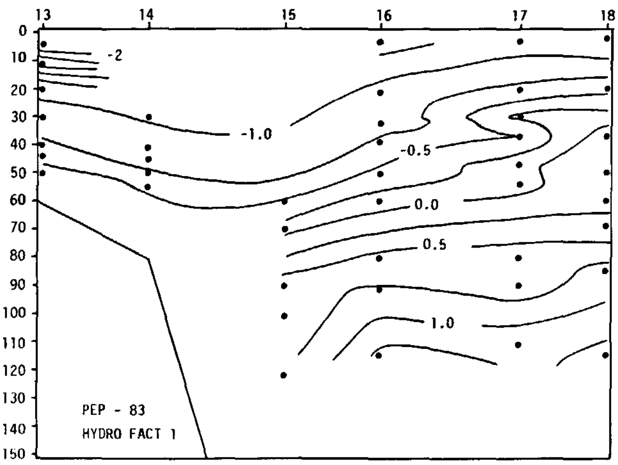

Figure 5

Spatial distribution of scores for the first component of the PCA on hydrographical data between stations 13 *and* 18 (see *Fig.* 1).

Répartition spatiale sur la radiale de stations 13 à 18 (*voir* fig. 1) des valeurs de la première composante (« scores ») de l'analyse des données hydrologiques.

OBSERVATIONS AND RESULTS

Description of the shelf/slope region

An in-depth analysis of the physical characteristics of the shelf/slope region can be found in Tintoré *et al.* (1989). However, a brief description is given here for the sake of completness. In the first part of the cruise (stations 1 through 36), a body of low-salinity water was found over the shelf (Fig. 4). The core of the low-salinity water (< 37.2) occupied the upper layer, from the surface to 40 m (station 22). In the slope region, the density front was detected (isopycnals deepening 40 m over a distance of 25 km), while near the coast, an even steeper upward lift of isopycnals was observed.

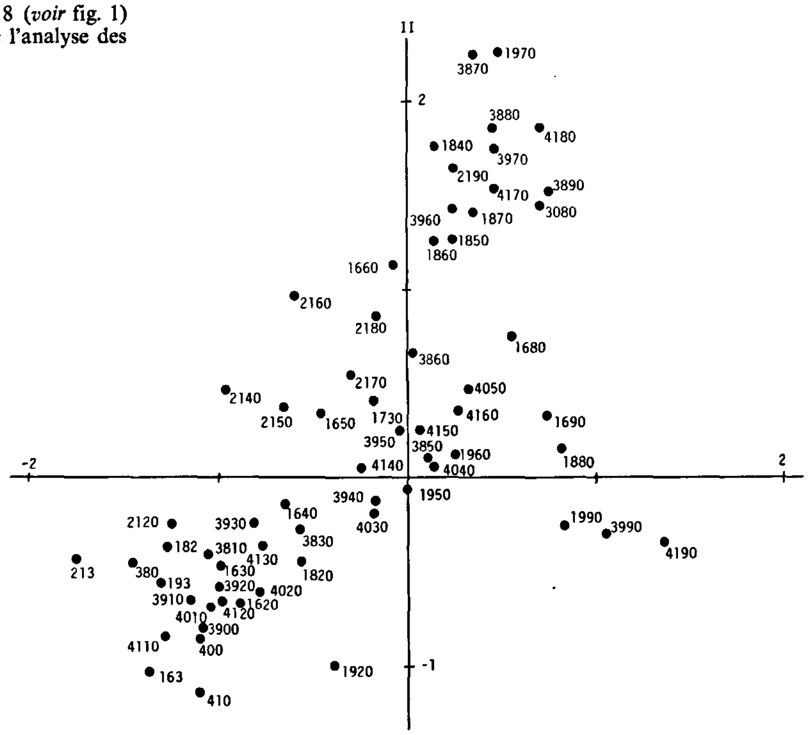

Figure 6

Distribution of samples from stations 16, 19, 18, 21, 38, 39, 40 *and* 41 *on the first plane of the PCA of hydrographical data. The first couple of numbers indicate the station, the second the depth.*

Distribution d'échantillons des stations 16, 19, 18, 21, 38, 39, 40 et 41 sur le plan des deux premiers axes de l'analyse en composantes principales des données hydrologiques. Les deux premiers numéros indiquent la station; les suivants la profondeur.

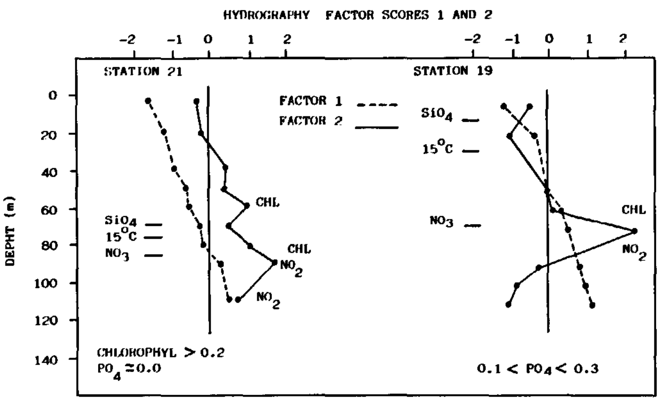

Figure 7

Profiles of the first and second component of the PCA of hydrographical data for stations 21 and 19. Maxima of factor 2 are due to chlorophyll and nitrite. The depths of 1 µM nitrate and silicate and of the 15°C isotherm are indicated by horizontal segments. At the bottom, mean values of chlorophyll and phosphate for the surface samples in these two stations are given.

Profils des deux premières composantes (scores) de l'analyse des données hydrologiques pour les stations 21 et 19. Les maximums du deuxième facteur indiquent des valeurs relativement grandes de chlorophylle ou de nitrite. Les segments horizontaux indiquent la profondeur où se trouvent les niveaux de 1 µM de nitrate et silicate et l'isotherme 15°C. En bas, les valeurs moyennes de phosphate et chlorophylle en surface sont données pour chacune des stations.

In the core of the less saline water, in the vicinity of stations 14, 15, 26 and 27, isohalines and isopycnals were almost parallel, suggesting that no significant shear stresses were present. Between this zone of low-salinity water and the slope front, frequent salinity inversions were found (*e.g.* stations 16, 17 and 28), suggesting that significant horizontal and vertical mixing occurred. This complex structure of interleaving layers was also detected in the vertical distributions of the first component of the PCA performed on the hydrographic data (Fig. 5).

Tintoré *et al.* (1989) showed that the low-salinity water found over the shelf was part of an anticyclonic eddy. This eddy, formed as a tongue of low-salinity cold water, originated in the northern Gulf of Lions and, moving southward in the slope region, turned anticyclonically off Barcelona.

Some of the samples were plotted on the first plane of the PCA of hydrographical data (Fig. 6). The relative distribution of the samples belonging to the same levels in the photic zone indicates that significant upwelling occured at station 19 (highest positive correlation with the first component and negative correlation with the second). PCA scores and the depth levels reached by

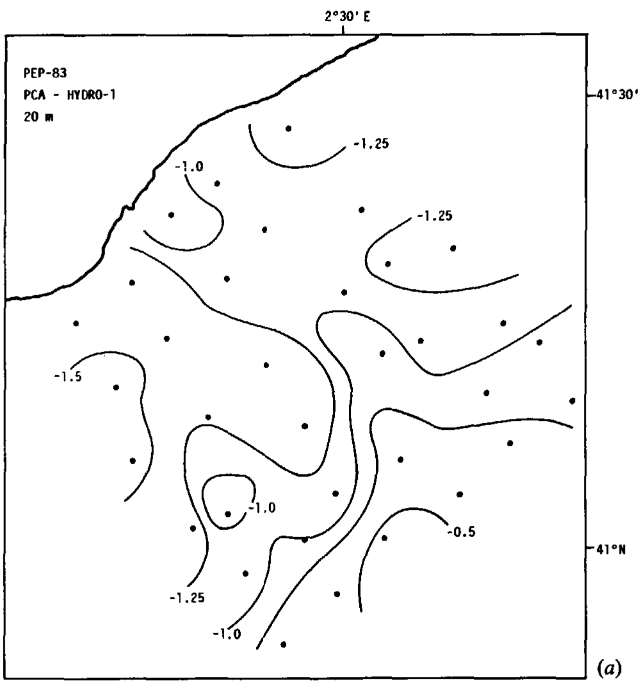

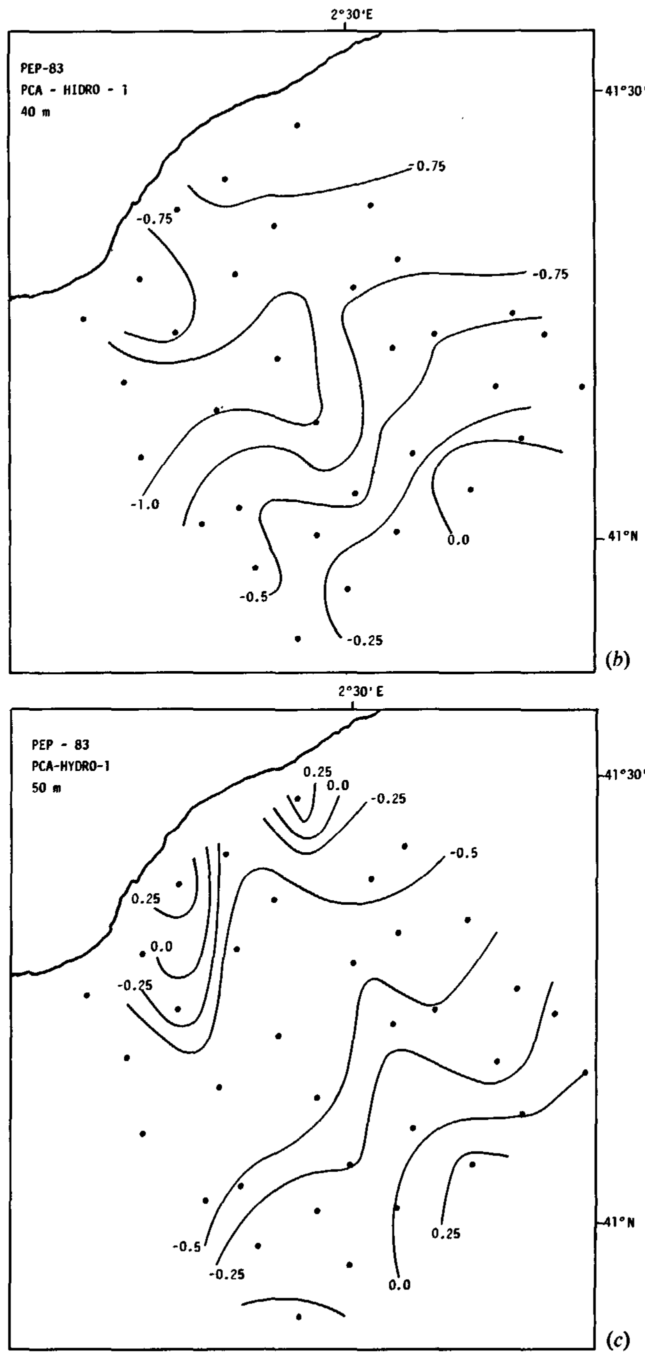

Figure 8

Horizontal distribution of the scores for the first component of the PCA of hydrographical data, at 20, 40 and 50 m depth (see text).

Répartition horizontale des valeurs de la première composante de l'analyse des données hydrologiques, à 20, 40 et 50 m de profondeur.

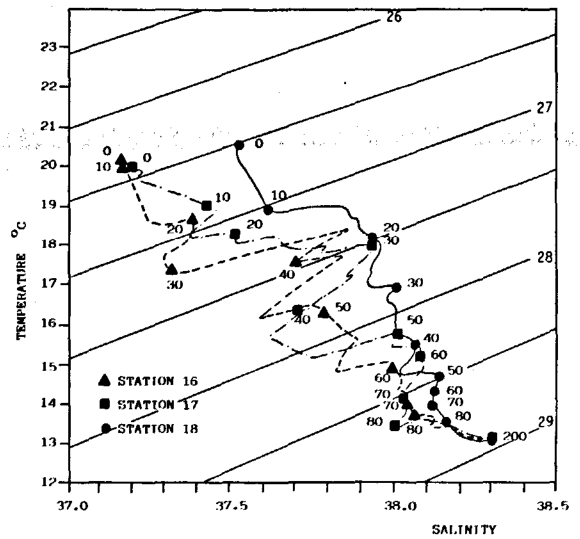

Figure 9
T-S diagram for stations 16, 17 *and* 18 (see *text*).
Diagrame T-S pour les stations 16, 17 et 18 (*voir* le texte).

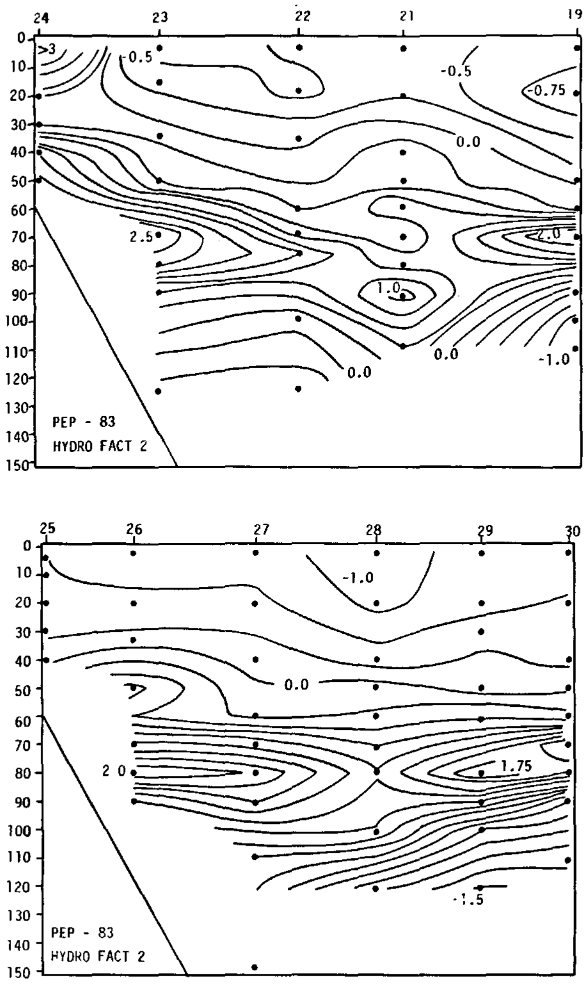

Figure 10
Distribution of the scores for the second component of the PCA of hydrographical data on two sections from the coastal grid of stations. Higher positive values are indication of chlorophyll and nitrite maxima.
Répartition de la deuxième composante de l'analyse des données hydrologiques sur deux radiales du réseau côtier de stations. Les maximums indiquent des valeurs relativement hautes de chlorophylle et de nitrites.

the 1 µM isolines of silicate and nitrate, as well as the depth of the 15°C isotherm, are shown for stations 21 and 19 in Figure 7. The horizontal distributions of the same first component at 20, 40 and 50 m (Fig. 8) suggest an onshore intrusion of waters from stations 18 and 19 to stations 17 and 16, and from stations 30 and 31 to stations 29 and 28, while the low-salinity water remains wedged between the two. On the shore side, uplifted water was found to extend from station 24 to station 26. Associated withe the frontal intrusions, strong surface convergence had to occur. This is confirmed by TS diagrams that indicate that water from 20 m at station 18 deepened to 30 m at station 17 and was detected at 40 m at station 16 (Fig. 9).

The second component issued from the PCA of hydrographical data is a good indicator of biological activity, since positive values are associated with high values of chlorophyll or nitrite. The vertical distribution of this component (Fig. 10) shows two separate maxima (onshore and offshore), at points where the nutricline reaches the highest levels. Another maximum observed in surface waters off Barcelona (station 24) is due to local enrichment by coastal runoff.

Silicate distribution (Fig. 11) also shows the two upwelling areas, one at the frontal edge, the other near the coast. Upwelled water mixes with the core of less saline water, producing a complex three-dimensional structure. The distribution of seston reflects the same overall hydrographical structures with an even greater spatial heterogeneity. Aphotic waters are characterized by low concentrations of particles and of chlorophyll and by high concentrations of nutrients. Samples well inside the photic zone, with low concentrations of both particles and chlorophyll (similar numbers to those found in the aphotic waters) and a relatively high concentration of silicate, reflect the presence of recently upwelled waters. On the other hand, low chlorophyll but high seston values are indicative of nutrient-depleted surface waters or of aphotic waters with a high input of sedimented material. In Figure 12 we show the distribution of seston concentration with an indication of points where chlorophyll is higher than 0.75 µg/l and points (marked A in the figure) where low seston concentration goes with very low values of chlorophyll (less than 0.1 µg/l) and relatively high silicate concentration (around 1 µM). Maxima of oxygen were found in the photic layer coinciding with silicate relative maxima at stations 17, 18 and 29, well above the chlorophyll maxima (Estrada and Salat, in press).

The main characteristics of the 7 groups of samples defined through the cluster analysis are shown in Table 1 and Figure 3. Groups 6 and 5 are surface waters. Groups 2 and 7 are found around 45 m. Groups 1 and 4 are near or belong to the deep chlorophyll maximum (DCM). Group 3 comprises samples from below the pycnocline.

A high heterogeneity is found between 20 and 80 m depth. Differences in the size spectra of seston suggest that the different factors involved in the shaping of the size distribution of particles play important roles in the studied area. Among these factors, nutrient and light levels must be significant, but so are the origin of the mixing waters, chance for the biological seeds and elapsed time (Margalef, 1969). Groups 2 and 7, for example, correspond to samples from the same depth, with similar temperatures and salinities, but the samples from group 7 are in all likelihood more productive (higher oxygen) than those in group 2. Seston particles in group 7 are smaller, and their mean chlorophyll content per particle or per unit seston volume is higher than for group 2. The correlation between size-class volumes and chlorophyll (Fig. 3) suggests that samples from group 2 have a population of phytoplankton cells around 10 µm equivalent diameter, which is absent from group 7 samples. Thus, it is likely that significant ecophysiological and taxonomic differences exist between the two sets of populations (the slight differences in nutrient concentrations may also reflect this).

All the size spectra (Fig. 3) show a higher proportion of seston volume around channel 8 (15-20 µm equivalent diameter). The lack of positive correlation between seston volume in these central size intervals and chlorophyll, as well as the negative correlation found between

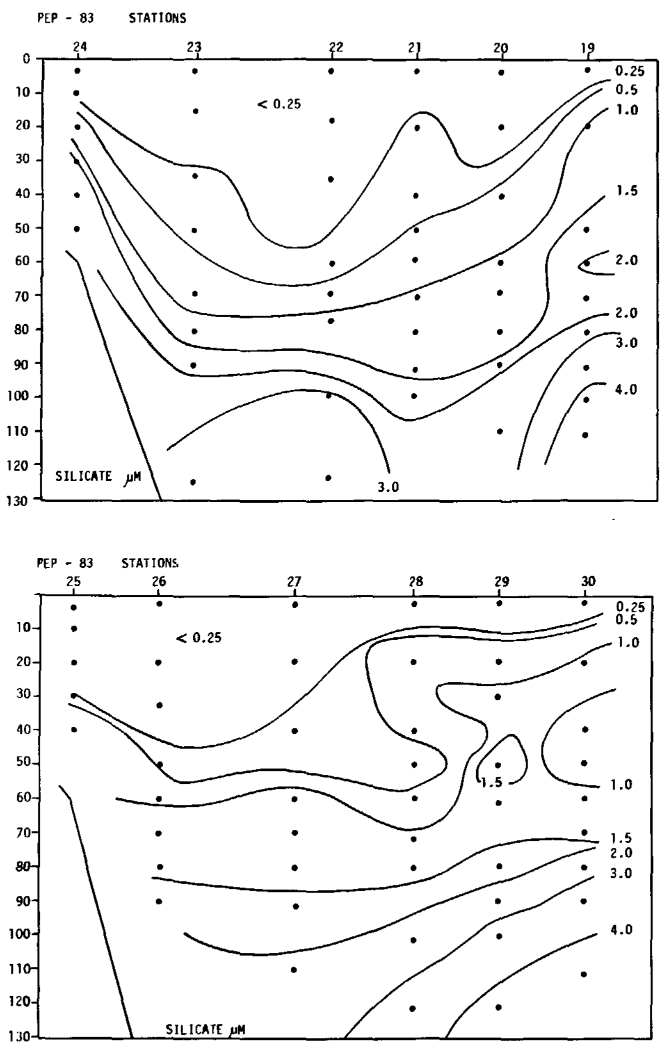

Figure 11

Spatial distribution of silicate concentration (µM) on two sections from the coastal grid of stations.

Répartition de la concentration en silicate (µM) sur deux radiales du réseau côtier de stations (*voir* fig. 1).

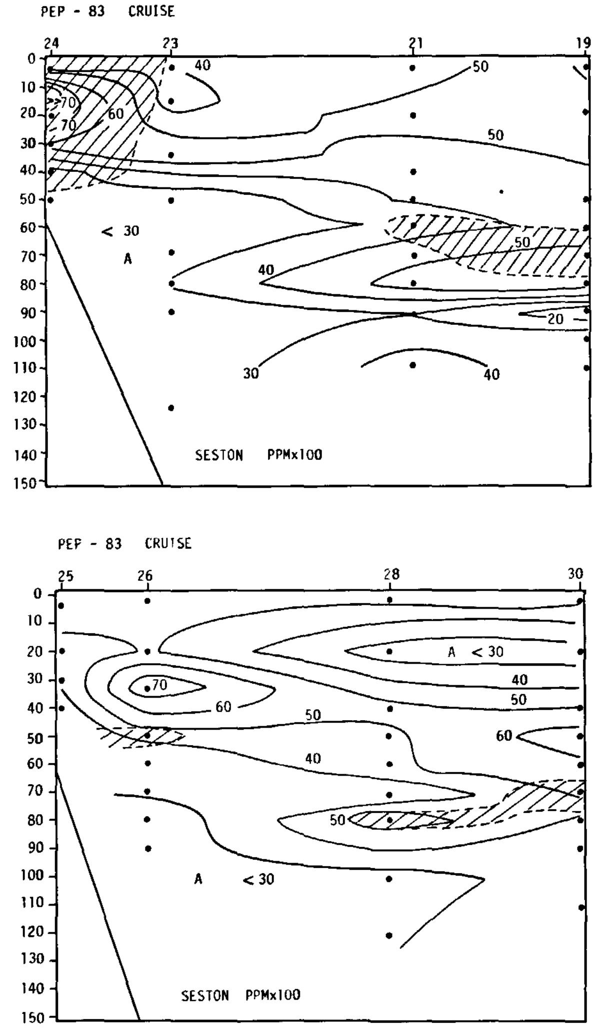

Figure 12

Distribution of seston concentration (ppm × 100, volume of particles between 3 and 80 µm equivalent diameter). Dashed areas have chlorophyll concentration higher than 0.75 µg/l. Points indicated by an A have low concentration of particles and silicate concentrations higher than 1 µM.

Répartition de la concentration de seston (ppm × 100, taille des particules comprises entre 3 et 80 µm de diamètre équivalent). Les zones hachurées indiquent une concentration en chlorophylle supérieure à 0,7 µg/l. La lettre A indique les régions avec une faible teneur en particules et une concentration de silicate supérieure à 1 µM.

these channels and the particulate organic carbon to nitrogen ratio (unpublished data), show that the central peak of the spectra is mainly detritic.

The central region of the Balearic Sea

From 4 to 16 July, two cross-sections were carried out between Barcelona and the Menorca Channel (station numbers higher than 36, Fig. 1). The two transects (stations 37 to 45, section A, and 86 to 75, section B) show a similar structure. Two regions where an uplift of nutrient-rich waters was detected were observed at the outer edges of the density fronts located near stations 39 and 42 (Fig. 13 and 14).

Section A shows that the low-salinity shelf waters have moved offshore (Fig. 13 *a*). The 30 m sample taken at station 39 had a salinity of 37.58 and no detectable

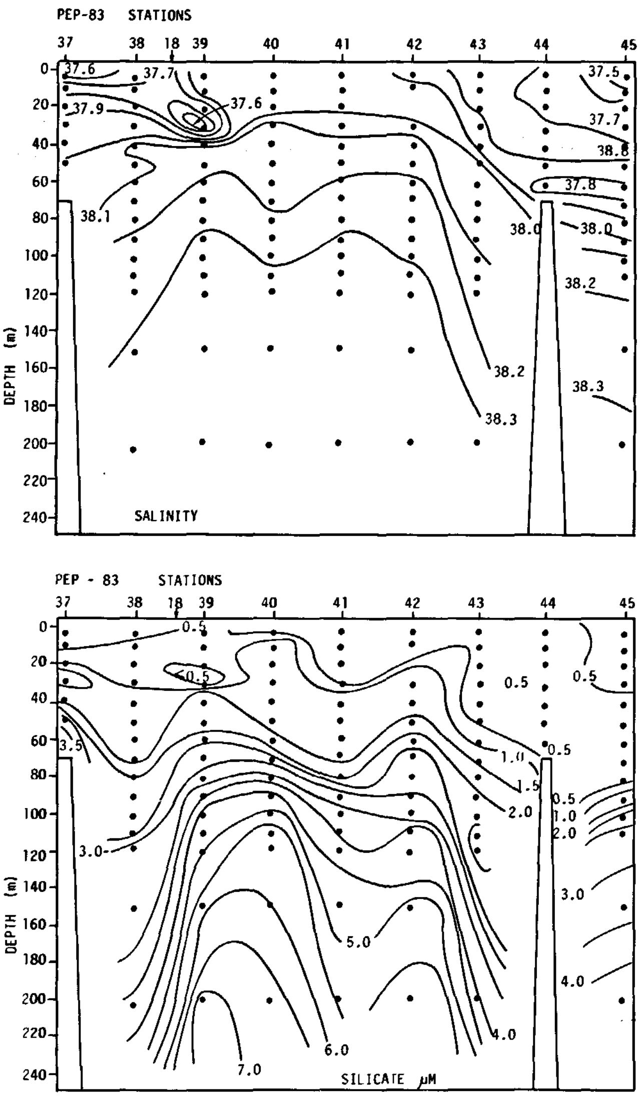

Figure 13

Distribution of salinity (a) and silicate (b) in the offshore stations after the sampling made between 3 and 5 July 1983.

Répartition de la salinité (*a*) et du silicate (*b*) pour les stations du large entre les 3 et le 5 juillet 1983.

silicate. T-S diagrams from stations 38, 39 and 40 (Fig. 15) suggest that a wedge of low-salinity water had subducted offshore, sinking from 15 m (at station 38) to 25 m (at station 39). Figure 13 indicates that there was vertical mixing at station 40, between waters raised under station 39 that upwelled offshore, and surface waters moving onshore from station 40 to station 39. Note that the 28.5 isopycnal found at 50 m at station 39 is found around 35 m at station 40 (Fig. 15). Thus, the uplift of isopycnals that was closer to station 18 some days earlier, moved offshore to station 40 and was substituted by a surface convergence.

Figure 16 shows the distribution of seston volume in the offshore stations. It can be seen that the concentration of particulate matter on 4 July (section A) is in general higher than twelve days later (section B), and its spatial distribution looks rather different. In the first leg, a relative maximum (centered at station 40) is found above the deep seston and chlorophyll maxima. Samples here were classified as belonging to group 1 (Table, Fig. 3). The relative seston maxima found in the DCM (Fig. 16) correspond to group 2 at station 38 and to group 4 at station 41. These two groups have in common a relative maximum of particles around 10 µm, positively correlated with chlorophyll. The DCM maxima were produced by diatoms, while the maximum above the DCM at station 40 is characterized by flagellate and dinoflagellate taxa (Estrada and Salat, in press). It is likely that the upwelled water enhanced the production of particles. The seaward spreading (at around 30 m) of this body of water represents an effective mechanism exporting nutrients and newly produced organic particulate matter towards the open ocean. Twelve days later (section B), the relative maximum of seston is centered on the island side, extending to the central zone of the Balearic Sea; but it is poorer and clearly disconnected from the coastal processes in front of Barcelona.

DISCUSSION

We have shown that in July 1983, nutrient-rich regions were detected near the coast, and in the photic layer on the deep ocean side of the two density fronts present in the Balearic Sea. Over the shelf, the low-salinity eddy was trapped against the coast and rotating, therefore inducing the observed coastal upwelling (Tintoré *et al.*, 1990). On the open ocean side, nutrient-rich regions have been also detected in other frontal studies (Boucher *et al.*, 1987) and are induced by the cross-

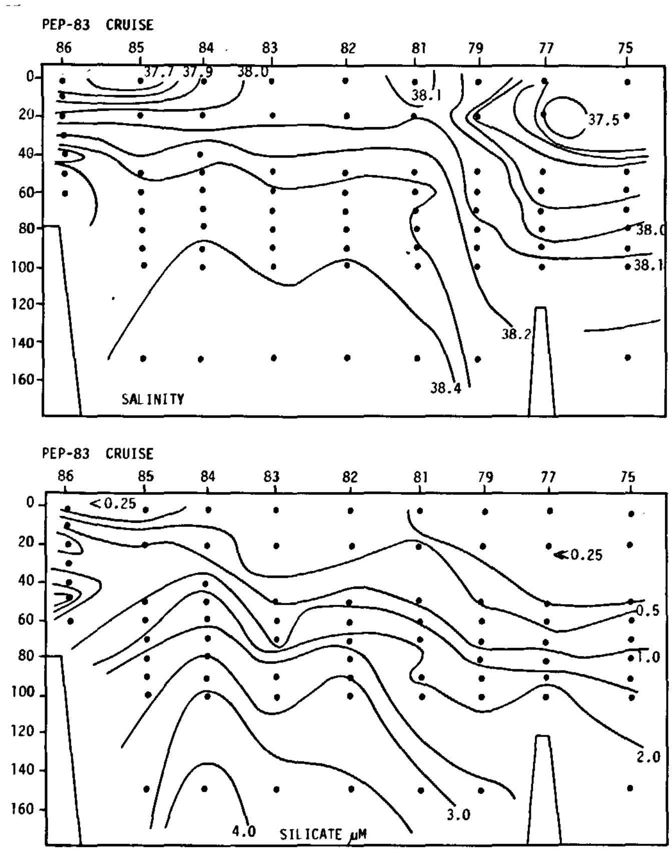

Figure 14

Distribution of salinity (a) and silicate (b) in the offshore stations after the sampling made between days 15th and 16th of July 1983.

Répartition de la salinité (*a*) et du silicate (*b*) pour les stations du large les 15 et 16 juillet 1983.

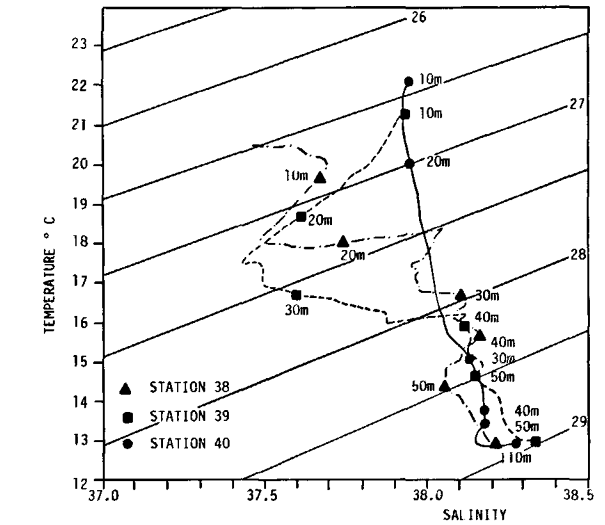

Figure 15
T-S diagram for stations 38, 39 *and* 40 (see *text*).
Diagrame T-S pour les stations 38, 39 et 40 (*voir* le texte).

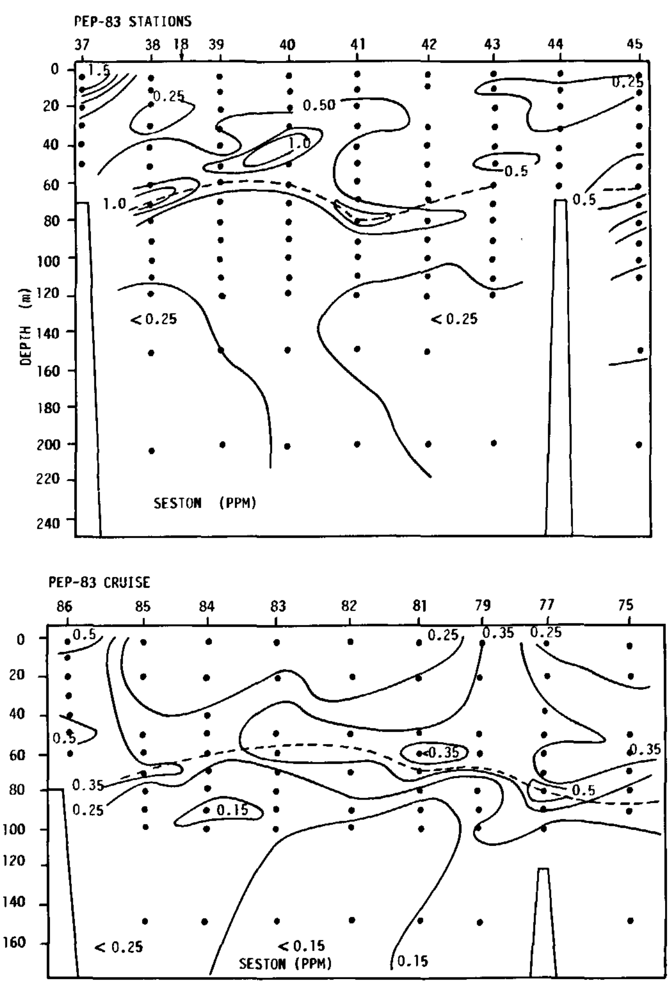

Figure 16
Distribution of seston (ppm) in the offshore stations between Barcelona and the Menorca Channel (a: 3rd to 5th July; b: 15th to 16th July). The deep chlorophyll maximum (DCM) is indicated by a dashed line (see *also Fig.* 13 *and* 14).
Répartition du seston (ppm) sur les stations situées entre Barcelone et le canal de Minorque (A : entre le 3 et le 5 juillet; B : les 15 et 16 juillet; *voir* aussi les figures 13 et 14). En pointillés, le niveau du maximum profond de chlorophylle.

frontal circulation that appears in density fronts as a result of non-linear and frictional effects (Mooers, 1978). This suggests that the two density fronts (not a central divergence) are responsible for the increased biological activity. Other studies in the Balearic Sea have focused attention on the central ridge or divergence (*e.g.* Margalef and Estrada, 1987) and therefore the distribution of stations was too coarse to detect either the two fronts or the regions of highest fertilization associated with them. However, it is important to note that these regions appear in almost any data set obtained in the region, although the sampling strategy and contourning procedures often led to somehow confusing pictures where the two doming structures associated with the fronts fuse into a large scale central doming (Estrada, 1985).

We have shown that the nutrient enrichment associated with the front on the continental side was followed by an offshore exportation of materials. The particulate matter found above the DCM at station 40 (midway from the continental coast to the Balearic Islands) is certainly associated to the nutrients upwelled in the front. This particulate matter is bound to sediment and recycle in the offshore waters, thus feeding the deeper layers from above. Other mechanisms or physical interactions might contribute to the existence of strong mixing or upward motion in the central region. For example, eddies and filaments associated with the Catalan front have been frequently observed (La Violette *et al.*, 1989; Masó, 1989), and Wang *et al.* (1988) showed that strong vertical motions were associated with them. Therefore the contribution of the permanent doming structure to the fertility of the Western Mediterranean estimated by Estrada and Margalef (1988) (85 mg P m^{-2} $year^{-1}$, or 34 % of the total new production) should be revised, since it has been shown that the fertilization occurs mainly at the two density fronts.

CONCLUSION

The presence of two highly dynamic, permanent density fronts suggests that the enrichment of the central part of the Balearic Sea in summer may be much more important than previously thought. This enrichment occurs in association with the cross-frontal ageostrophic circulation and with transient but very energetic instabilities (eddies or filaments) that are themselves associated with the fronts. A fresh estimation of the new production in the Western Mediterranean should be based on an accurate characterization of the spatial and temporal scales of these two physical mechanisms.

Acknowledgements

The authors wish to thank Dr. J. Romero who was in charge of the Coulter counter measurements during the first leg of the cruise. Thanks are also due to A. Domingo for assistance with the drawings. This work was supported by CAICYT grant 2311308 and CICYT 87087-CSIC.

REFERENCES

Allain C. (1960). Topographie dynamique et courants généraux dans le bassin occidental de la Méditerranée. *Revue Trav. Inst. Pêches Marit.*, **24**, 1221-145.

Boucher J., F. Ibanez and L. Prieur (1987). Daily and seasonal variation in the spatial distribution of zooplankton populations in relation to the physical structure in the Ligurian Sea Front. *J. mar. Res.*, **45**, 133-173.

Dugdale R. C. and J. J. Goering (1967). Variations in photosynthetic assimilation ratios in natural, marine phytoplankton communities. *Limnol. Oceanogr.*, **12**, 2, 196-206.

Estrada M. (1985). Deep Phytoplankton and Chlorophyll maxima in the Western Mediterranean. In: *Western Mediterranean Ecosystems*, Moraitou-Apostolopoulou, M. and V. Kiortsis, Editors, Plenum Press, New York and London, 247-277, 407 pp.

Estrada M. and R. Margalef (1988). Supply of nutrients to the Mediterranean photic zone along a persistent front. *Océanographique pélagique méditerranéenne, Oceanologica Acta*, **n° sp.**, 133-142.

Estrada M. and J. Salat (in press). Phytoplankton assemblages of deep and surface water in a Mediterranean frontal zone. *22nd Marine Biology Symposium Proceedings.*

Flos J. (1976). Seston superficial de la zone de afloramiento del NW de Africa. *Oecol. aquat.*, **2**, 27-39.

Flos J. (1979). Interpretación de varios análisis de las componentes principales aplicados a un conjunto de datos oceanográficos de una zona neritica del Golfo de Vizcaya. *Investigación pesq., Barcelona*, **43**, 611-635.

Flos J. (1980). Material en suspensió oceànic i la seva distribució en el Mediterrani Occidental. *Ph. D. Thesis, University of Barcelona*, 342 pp.

Flos J. (1987). Data analysis in pelagic community studies. In: *Developments in Numerical Ecology*, P. Legendre and L. Legendre Editors, NATO Advanced Study Institute Series G. (Ecological Sciences), Springer-Verlag, Berlin, 494-520.

Font J., J. Salat and J. Tintoré (1988). Permanent features in the circulation of the Catalan Sea. *Océanographie pélagique méditerranéenne, Oceanologica Acta*, **n° sp.**, 51-57.

Grup PEPS (1986). Datos oceanográficos de las campañas PEP-82, PEP-83 y PEP-84 en el Mar Catalán. Datos informativos, 19. Institut de Ciències del Mar, Barcelona, 100 pp.

Jacques G., H. J. Minas, M. Minas and P. Nival (1973). Influence des conditions hivernales sur les productions phyto- et zooplanctoniques en Méditerranée nord-occidentale. II : Biomasse et production phytoplanctonique. *Mar. Biol.*, **23**, 251-265.

Jacques G., M. Minas, J. Neveux, P. Nival and G. Slawyk (1976). Conditions estivales dans la divergence de Méditerranée nord-occidentale. III : Phytoplancton. *Annls Inst. océanogr., Paris*, **52**, 141-152.

Kitchen J. C., D. Menzies, H. Pack and J. R. V. Zaneveld (1975). Particle size distribution in a region of coastal upwelling analysed by characteristic vectors. *Limnol. Oceanogr.*, **20**, 775-783.

La Violette P., J. Tintoré and J. Font (1990). The surface circulation of the Balearic Sea, *J. geophys. Res.* (in press).

Legendre L. and P. Legendre (1983). *Numerical Ecology*. Elsevier, Amsterdam.

Margalef R. (1969). Small scale distribution of phytoplankton in Western Mediterranean at the end of July. *Publ. Staz. zool. Napoli, suppl.*, **37**, 40-61.

Margalef R. and M. Estrada (1987). Synoptic distribution of summer phytoplankton (Algae and Protozoa) across the principal front in the Western Mediterranean. *Investigación pesq., Barcelona*, **51**, 121-140.

Masó M. (1989). Variabilidad espacio-temporal de las características oceanográficas de la zona costera y su relación con el sistemo planctónico. *Ph. D. Thesis, University of Barcelona.*

Mooers C. N. K. (1978). Frontal dynamics and frontogenesis. In: *Oceanic fronts in coastal processes*. B. M. Bowman and W. E. Essais, Editors, Springer-Verlag, 16-22.

Ovchinnikov I. M. (1966). Circulation in the surface and intermediate layers of the Mediterranean. *Oceanology*, **6**, 48-59.

Prieur L. and M. Tiberti (1985). Identification et échelle des processus physiques et biologiques responsables de l'hétérogénéité spatiale près du front de Mer Ligure. *Rapp. P.-V. Réun. Commn. int. Explor. scient. Mer. médit.*, **29**, 35-36.

Sheldon R. W. and T. R. Parsons (1967). A practical manual on the use of the Coulter counter in marine research. Coulter electronics, Toronto, 66 pp.

Sournia A. (1973). La production primaire planctonique en Méditerranée. Essai de mise à jour. *Bull. Étude commun Médit.*, **5**, 1-128.

Tintoré J., D.-P. Wang and J. La Violette (1990). Eddies and thermohaline intrusions on the shelf/slope front off the northeast Spanish coast, *J. phys. Oceanogr.* (in press).

Wang D. P., M. Vieira, J. Salat and J. Tintoré (1988). A shelf/slope frontal filament off the Northeast Spanish coast. *J. mar. Res.*, **46**, 321-332.

Ward J. H. (1963). Hierarchical grouping to optimize an objective function. *J. Am. Stat. Assoc.*, **58**, 236-244.